DESIGN OF THE JINR FOUR-METER ISOCHRONOUS CYCLOTRON WITH SMOOTHLY REGULATED HEAVY-ION ENERGIES

I. A. Shelaev, E. D. Vorob'ev,
B. A. Zager, S. I. Kozlov,
V. I. Kuznetsov, R. Ts. Oganesyan
Yu. Ts. Oganesyan, K. I. Semin,
A. N. Filipson, and V. A. Chugreev

Further development in the physics of nuclear reactions between complex nuclei is bound up with the use of fast ion beams of even heavier elements in these reactions and also with an increase in their energy and intensity. For this purpose, a four-meter isochronous cyclotron (accelerator U-400) has been designed in the JINR Laboratory of Nuclear Reactions on the basis of the results obtained in the construction of the JINR two-meter isochronous cyclotron U-200 [1]. At the present time, work at JINR involves the fabrication of parts and sections of the U-400 accelerator, which is being built on the foundations of the existing 310-centimeter, classical heavy-ion cyclotron (accelerator U-300) [2].

The parameters of these accelerators are given in Table 1, from which it is apparent that practically all the systems of the U-400 accelerator differ significantly from those of the U-300. The U-400 cyclotron is very much like the U-200 accelerator, which can be considered as a model of the larger accelerator on
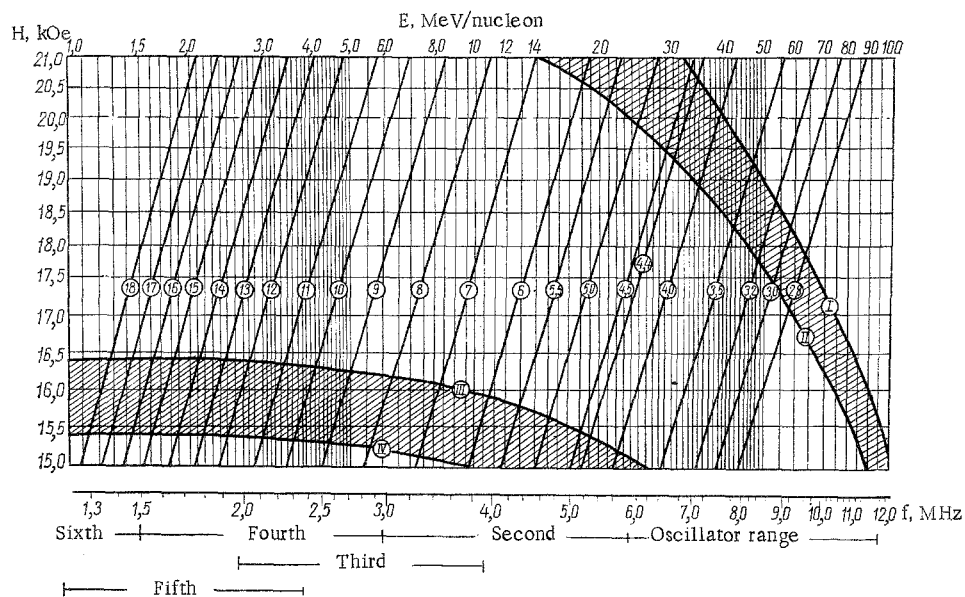

Fig. 1. Energy of ions with various values of A/Z (numbers in circles) in the operating range of the levels of the average field H and rotational frequency f of the ions at the final radius $R_f = 180$ cm for the U-400 cyclotron. The Roman numerals I-IV correspond to the values 0, 0.04, 0.21, and 0.25 for ν_z^2.
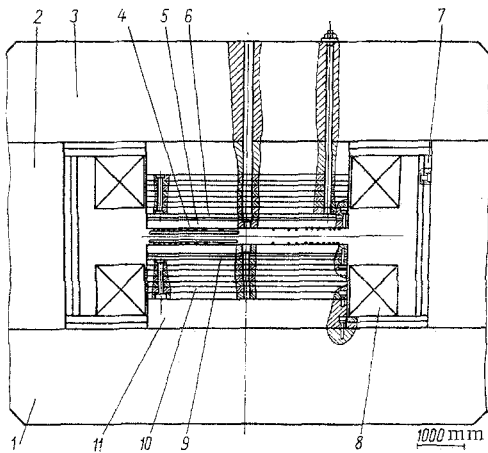
Fig. 2. Electromagnet of the U-400 cyclotron: 1, 3) upper and lower beams; 2) columns; 4) sector; 5) chamber cover; 6,9) upper and lower spacer discs; 7) supplementary iron yoke; 8) excitation coils; 10, 11) new and old pole stacks.

a 1:2 scale. Some differences primarily concern the magnetic field structure in connection with the expansion of the mass and energy of the accelerated ions. Figure 1 shows the energy E for ions with different A/Z and the rotational frequency of these ions in the selected range of working levels of the average magnetic field in the cyclotron (16-20 kOe at the final radius of 180 cm). In the figure, the hatched regions correspond to the areas where the breakdown of betatron oscillation stability arises. Expansion of the range of final energies of the ions accelerated in the cyclotron from E =5-10 to E =1-50 MeV/nucleon and of the range A/Z ratios from 5-7 to 3.5-25 are ensured by an increase in the magnetic field level, by the introduction of azimuthal variations, and by other changes in the cyclotron structure.

Magnet Structure

To increase the level of the magnetic field to 20 kOe, the cross section of the magnetic circuit of the electromagnet (Fig. 2) was increased by 13%, and the spacing between the main excitation coils was reduced by 500 mm. The conical pole tips (D_{max} =400 cm, D_{min} =310 cm) were replaced by cylindrical ones 400 cm in diameter. The new pole tips were built up from separate discs using the same technology as for the U-200 cyclotron [3]. The average air gap between the poles was reduced from 540 to 200 mm.

Magnetic circuit calculations and extrapolation of experimental results obtained with the U-200 cyclotron showed that after completion of the changes listed above, an average magnetic field of 20-20.5 kOe could be obtained with an excitation current of 2200-2500 A in the main coils. This made it possible to keep the old electromagnet supply system without change.

The magnetic gap of the U-400 cyclotron is shown in Fig. 3. The spacing between the steel vacuum chamber covers is 300 mm. The elements for shaping the magnetic field (sectors, concentric coils, etc). and the dees are located in this gap. These elements were designed with the results obtained on the U-200 cyclotron kept in mind. The isochronous shape of the magnetic field is determined by the expression

$$H_{is} = \frac{H_0}{\sqrt{1 - \frac{2W}{E_0}}} ,$$

where W is the ion kinetic energy per nucleon and E_0^- is the proton rest energy; this shape is ensured by circular shims and concentric coils. The calculation of the required configuration of the circular shims was done on a computer. As experiments performed on the U-200 showed, the accuracy of these calculations is about 10% of the total shim contribution ($\sim$1.5 kOe); consequently, further field correction will be
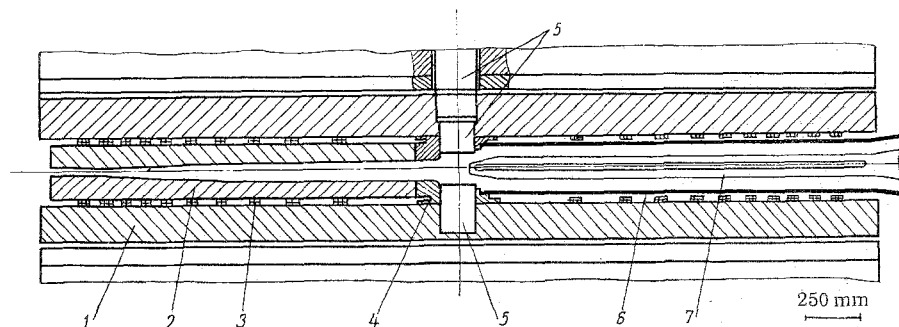

Fig. 3. Geometry of the air gap in the U-400 cyclotron: 1) steel chamber covering; 2) sector shim; 3) circular correction coil; 4) central shim; 5) removable central plugs; 6) chamber cladding; 7) dee.

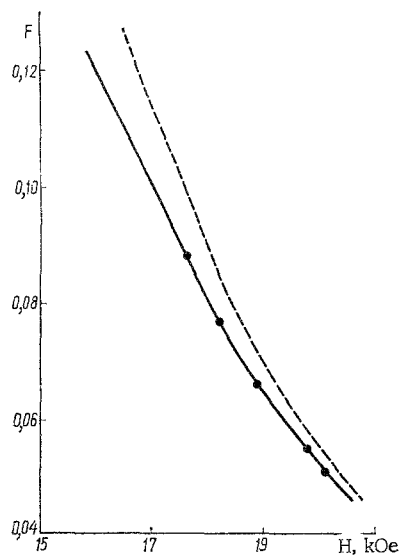Fig. 4   Fig. 5

Fig. 4. Dependence of the magnetic field flutter in the U-200 cyclotron
(———) and of the U-400 cyclotron flutter corrected for sector height (- - - -)
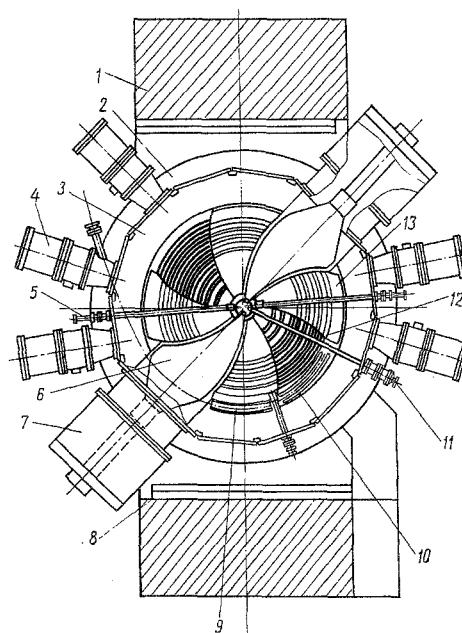on the average field level at the final radius of the accelerator.

Fig. 5. Diagram of U-400 accelerator: 1) electromagnet column; 2) excita-
tion coil; 3) vacuum chamber; 4) VA-8-4 high-vacuum pump; 5) transfer
probe; 6) dee; 7) resonator; 8) supplementary iron yoke; 9) magnetic chan-
nel; 10) electrostatic deflector; 11) ion source; 12) concentric coil; 13) sec-
tor shim.

accomplished experimentally. In the U-400 cyclotron, such shims are located only in the sectors and are
fabricated together with them. This type of shim arrangement complicates sector construction somewhat,
but makes it possible at the same time to reduce the height of the circular shims and simplifies their fabri-
cation technology.

Correction of the average magnetic field over the entire operating range of field levels is accom-
plished with concentric coils. Calculation of the ampere-turns required for correction was performed on
a computer by the least-squares method for two versions of radial coil distribution — uniformly in r and r^2.
To obtain an isochronous magnetic field shape and permissible radial gradients, the number of coil pairs
was varied from 8 to 12. It should be noted that for a coil distribution uniform in r^2, the ampere-turns for
each coil were nearly the same. The U-400 current-correcting system contains ten pairs of concentric
coils (total number of ampere-turns IW = 22,500). Each circular coil consists of three turns of a hollow
copper conductor 11.5 × 11.5 mm in size with a central opening 8 mm in diameter for cooling. The turns,
which were insulated with a fiber-glass-epoxy compound, were put down in an aluminum housing located
under the sectors (see Fig. 3).

Each concentric coil is fed from a six-phase silicon rectifier through a choke filter. Current regula-
tion (from 0 to 900 A) is accomplished by a magnetic amplifier connected in the primary circuit of a step-
down transformer. Separate supplies for the upper and lower coils are provided for three pairs of concentric
coils in order to achieve median plane corrections. Amplitude and phase control of the lower harmonics of
the magnetic field nonuniformity is accomplished by six pairs of azimuthal coils.

Azimuthal variation of the magnetic field is created by four sector pairs. The sector height and the
magnetic field flutter was calculated with the results obtained on the U-200 in mind. The proposed magnitude

TABLE 1. Parameters of the U-300 and U-400 Cyclotrons

System characteristic	U-300	U-400
Electromagnet		
Diameter of pole tips, cm	310	400
Final acceleration radius, cm	138	180
Magnet weight, tons	1900	2260
Average air gap, mm	540	200
Number of turns in main excitation coils	2×224	2×224
Operating current in electromagnet coil, A	1870	1000 — 2500
Average magnetic field, kOe	16,7	16 — 20
Number of sectors	—	4
Angle of spiral	—	30°
Radial drop in magnetic field, %	0,8	Isochronous
Number of auxiliary coils	4	19
Hf-system		
Number of dees	2	2
Azimuthal extent of dee	180°	45°
Dee voltage, kV	150	70—100
Wavelength range, m	50—100	25—50
Dee aperture, mm	40—140	80—40
Dee-chamber cladding gap, mm	80	70
Tunable element	Shorting plate	Movable panel
Dee voltage stability, %	None	0,2
Mode of operation	Pulsed	Arbitrary
Vacuum system		
Vacuum chamber volume, m³	75	25
Chamber pressure, mm Hg	$6 \cdot 10^{-6}$	$1 \cdot 10^{-6}$
Number of high-vacuum, oil-vapor pumps	5	5 (7)
Capacity of a single pump, sec⁻¹	20 000	8000
Extraction and Beam Transport systems		
Azimuthal extent of deflector, deg	103	45
Entrance and exit gaps, mm	8/22	6
Deflector working voltage, kV	40—60	40—60
Azimuthal extent of focussing magnetic channel, deg	34	45
Field gradient in channel, Oe/cm	450	1500
Number of extracted beams	1	2
Number of switching magnets	2	3
Number of working directions	12	16
Extraction efficiency, %	30	30—100
Beams		
Energy of accelerated ions, MeV/nucleon	5—10	1—50
Total energy, MeV	250 Z^2/A	400—625 Z^2/A
Mass-to-charge ratio A/Z	5—7	3,5—25
Energy spread, %	0,5	0,2—0,3

of the flutter as a function of the average magnetic field level at the final radius of the accelerator is shown in Fig. 4. Using these flutter values, the spiral angle of the sectors was chosen with consideration given to the following conditions. With the introduction of helicity, vertical focussing is increased and the allowance for shaping the magnetic field, particularly at high levels, is reduced. However, at large angles, the limits of field regulation are reduced because the quantity ν_z rises to 0.5 with a decrease in the field level. The sector helicity angle was chosen to be 30° so that $\nu_z \leq 0.5$ for ions with energies up to 5 MeV/nucleon at a magnetic field level of 16 kOe.

Thus the magnetic field structure selected for the U-400 cyclotron makes it possible to accelerate ions over a broad A/Z range and with smoothly controlled energy (see Fig. 1) without using flutter-correcting coils.

Magnetic Field Measurements

The increase in accelerator dimensions and the expansion in the range of magnetic field operating levels lead to an increase in the volume of magnetic measurements by almost an order of magnitude in comparison with the volume of measurements on the U-200 cyclotron [4]. In shaping the magnetic field of the U-200 cyclotron, the total number of measured field values was 400,000, which took about 300 h on the whole.

If the previous rate of measurement is retained, the performance of the magnetic measurements would require about 3000 h. This number includes only the time of actual measurement, and does not include the time which would be spent on the fabrication of the measured version of a shim, on the fabrication of equipment, etc. At the present time, work is going on to improve the measuring technique developed for the U-200 cyclotron for the purpose of increasing the rate of measurement by factors of three or four while maintaining, and even increasing, accuracy, and also for the purpose of increasing the reliability and recording speed of the measurements.

Hf-System

A diagram of the arrangement of the basic units of the U-400 accelerator is shown in Fig. 5. Preservation of the old electromagnet yoke makes the use of more than two dees difficult. The choice of frequency range (6-12 MHz) for the two-dee version was decided by the following conditions. First, the use of the amplitude of the accelerating voltage should be most efficient for the acceleration of ions with A/Z =7-12 (the heaviest for which there is the greatest interest). The maximum energy rise experienced by particles per turn in such a system is

$$\Delta E_{\max} = 4\overline{Z}_e U_g \sin \frac{n\pi}{8} \,,$$

where n is the order of the accelerating voltage harmonic. Second, the amplitude of the accelerating voltage should be such that breakdown in the chamber is practically completely eliminated for the selected
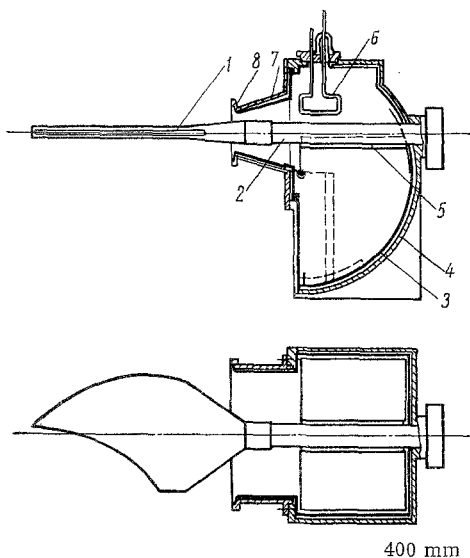
400 mm

Fig. 6. Model of U-400 cyclotron resonator: 1) dee; 2) stem; 3) resonator housing; 4) copper cladding of resonator; 5) movable panel in maximum frequency position (dashed lines show minimum frequency position); 6) coupling loop; 7) transition fitting; 8) flange.

TABLE 2. Energy and Intensity of Ions to be Accelerated in the U-400 Cyclotron

Type of ion accelerated	Energy, MeV /nucleon	Intensity of internal beam, particles/sec
Ne_{20}^{+2}	6,2	$9 \cdot 10^{14}$
Ne_{20}^{+3}	14,1	$4 \cdot 10^{14}$
Ne_{22}^{+3}	11,6	$4 \cdot 10^{14}$
Ar_{40}^{+5}	9,8	$6 \cdot 10^{13}$
Zn_{64}^{+7}	7,5	$2,5 \cdot 10^{13}$
Kr_{84}^{+8}	5,7	$1,8 \cdot 10^{13}$
Kr_{84}^{+9}	7,2	$1,3 \cdot 10^{12}$
Xe_{132}^{+12}	5,2	$5 \cdot 10^{11}$
Xe_{132}^{+13}	6,1	10^{11}

dee-chamber cladding gap (7 cm); this ensures stable machine operation in both continuous and pulsed modes. Finally, the third condition for the choice of frequency range was that it should be a multiple of the frequency range of the existing "Apatit" generator (f =3-6 MHz).

On this basis, an accelerator mode in the second-fourth harmonics was chosen for ions with A/Z =7-12 (see Fig. 1). With a dee voltage amplitude U_g =100 kV, these ions, accelerating to the final energy, will then complete about 200 revolutions. Increase in the number of revolutions and operation at higher harmonics of the ion rotation frequency require stabilization of the accelerating voltage amplitude to an accuracy of the order of ±0.2%. The frequency of the dee circuit is controlled in the given range by means of a moving panel.

The resonator model with a single rotating panel [5] selected for the U-400 cyclotron makes it possible to achieve changes in the frequency of the dee circuit by a factor of two comparatively simply. A model of the U-400 cyclotron resonator is sketched in Fig. 6. One edge of the rotating panel makes contact with the cladding of the resonator by means of a crimped copper plate, and contact of the second stage is provided by the capacity of the vacuum condenser formed by the shoe and the resonator wall. Measurements of resonator Q and impedance, made with a full-size model, showed that a dee voltage amplitude of 100 kV is provided at any frequency in the assigned range with generator power from 75-100 kW.

Ion Sources

The comparatively large gap between the vacuum chamber covers in the U-400 cyclotron (see Fig. 5) makes it possible to use ion sources in horizontal and vertical arrangements. Horizontally constructed sources are mainly intended for producing ions from elements which are normally only in the solid state because the chamber dimensions are increased in this case by the presence of a vaporizer for the working material, which is located in the immediate vicinity. A vertical opening in the electromagnet yoke permits the use of an ion source in a vertical arrangement [6, 7]; in addition, it can be used for the external injection of a beam of heavy ions from sources operating on other principles [8]. The arrangement of such sources in the accelerator chamber and their operation in the magnetic field of the cyclotron presents some difficulties.

Beam Extraction

Extraction of the beam from the U-400 cyclotron will be accomplished in two ways – by an electrostatic deflector and by charge-exchange of the ions in a thin foil [9, 10]. As experience with the U-200 has shown, the realization of these two methods encounters no fundamental difficulties; however, because of vaporization and erosion of the charge-exchange foils, the extraction of intense beams of heavy ions with A ≥ 40 by the charge-exchange method is limited.

Thus the increase in energy and the expansion of the range of A/Z ratios of the accelerated ions makes it possible to increase the intensity in beams of ions of standard elements (neon, argon) with mass

$A \leq 40$ because of acceleration in the isochronous mode of ions of the elements at lower charge, or to increase their energy by acceleration of ions with their previous charge, and, finally, to accelerate ions with a mass $A \leq 132$. Table 2 shows the intensity and maximum energy of various heavy ions which will be accelerated in the U–400 cyclotron.

LITERATURE CITED

1. I. A. Shelaev et al., JINR Preprint 9-3988, Dubna (1968).
2. V. S. Alfeev et al., JINR Preprint P-2693, Dubna (1966).
3. I. A. Shelaev et al., JINR Preprint P-9-4233, Dubna (1968).
4. E. G. Imaev et al., JINR Preprint 9-3713, Dubna (1968).
5. T. Johnson et al., IEEE Transactions on Nucl. Science, NS-16, 438 (1969).
6. K. W. Ehlers, Nucl. Instrum. and Methods, 18-19, 571 (1962).
7. T. Tauti et al., JINR Report 9-4368, Dubna (1969).
8. E. D. Donets et al., JINR Preprint P7-4124, Dubna (1968).
9. I. A. Shelaev et al., JINR Preprint P9-4831, Dubna (1969).
10. I. A. Shelaev et al., JINR Report P9-5037, Dubna (1970).